Investigation of Plasma Detachment from a Magnetic Nozzle

Except where reference is made to the work of others, the work described in this thesis is my own or was done in collaboration with my advisory committee. This thesis does not include proprietary or classified information.

William Chancery

Certificate of Approval:

David Cicci
Professor
Aerospace Engineering

Roy Hartfield, Chair
Professor
Aerospace Engineering

Edward Thomas, Jr.
Associate Professor
Physics

Joe F. Pittman
Interim Dean
Graduate School

Investigation of Plasma Detachment from a Magnetic Nozzle

William Chancery

A Thesis

Submitted to

the Graduate Faculty of

Auburn University

in Partial Fulfillment of the

Requirements for the

Degree of

Master of Science

Auburn, Alabama
August 4, 2007

Investigation of Plasma Detachment from a Magnetic Nozzle

William Chancery

Permission is granted to Auburn University to make copies of this thesis at its discretion, upon the request of individuals or institutions and at their expense. The author reserves all publication rights.

_____

Signature of Author

_____

Date of Graduation

Thesis Abstract

Investigation of Plasma Detachment from a Magnetic Nozzle

William Chancery

Master of Science, August 4, 2007
(B.S., Auburn University, 2002)

52 Typed Pages

Directed by Roy Hartfield

The Variable Specific Impulse Magnetoplasma Rocket (VASIMR) electric space propulsion concept currently under development by the Ad Astra Rocket Company utilizes a magnetic field to confine a propellant plasma. The energetic ions in the plasma are converted into a directed exhaust flow by a magnetic nozzle. The interaction between the diverging magnetic field and the escaping plasma plume is of interest both because of its technological importance in this application and its relationship to naturally occuring phenomena in the field of space plasma physics. The research presented here was carried out at the Propulsion Research Center of Marshall Space Flight Center. The focus of this effort is the measurement of the time dependent effect of a plasma plume on the vacuum magnetic field geometry in a simulated magnetic nozzle. Data was gathered with magnetic field probes constructed at the Royal Institute of Technology in Stockholm, Sweden. This data was analyzed and compared to published theoretical descriptions of plasma detachment from a magnetic nozzle. The results of that analysis are presented here.

Acknowledgments

Thanks go to Franklin Chang-Díaz and the Ad Astra Rocket Company for supporting this research, Greg Chavers and the Propulsion Research Center at Marshall Space Flight Center for providing the environment and apparatus, and Einar Tennfors and Nils Brenning at the Alfvén Institute of the Royal Institute of Technology in Stockholm for constructing the probes used.

Style manual or journal used AIAA

Computer software used The document preparation package TEX (specifically LATEX) together with the Auburn style-file `aums.sty`. The mathematical software Matlab®was used for data processing and generating plots.

Table of Contents

List of Figures

Chapter 1

Project Description

The Variable Specific Impulse Magnetoplasma Rocket (VASIMR) is a high power electric space propulsion concept under development by the Ad Astra Rocket Company (AARC) at Johnson Space Center. The concept for the VASIMR engine was developed by Dr. Franklin Chang Díaz as an outgrowth of research in magnetically contained fusion plasmas.[1] The development of the propulsion system was initiated at the Massachussetts Institute of Technology in the early 1980's and later transferred to Johnson Space Center when Dr. Chang Díaz joined the Astronaut Corps.[2,3] The VASIMR engine utilizes a magnetically contained plasma heated by radio waves to produce thrust. The rocket design can be split into three separate magnetic sections or cells. In the forward section neutral propellant gas is injected and ionized by radio waves from a helicon antenna.[4] The bulk of the RF power is directed to the Ion Cyclotron antenna in the middle section of the engine where the power is absorbed by the ions.[5] The last cell is the magnetic nozzle which converts the thermal energy of the plasma into a directed exhaust flow. It is here that the reaction force between the energetic ions and the confining magnetic field coils occurs. This interaction accelerates the ions with respect to the engine structure and is the ultimate source of the thrust generated by the rocket. Figure 1.1 presents a schematic view of the VX-10 which is a laboratory experimental prototype of the VASIMR engine with a total power rating of 10kW.[6]

This thesis concentrates on the related Detachment Demonstration Experiment (DDEX) that took place at Marshall Space Flight Center under the direction of Greg Chavers.[7] This

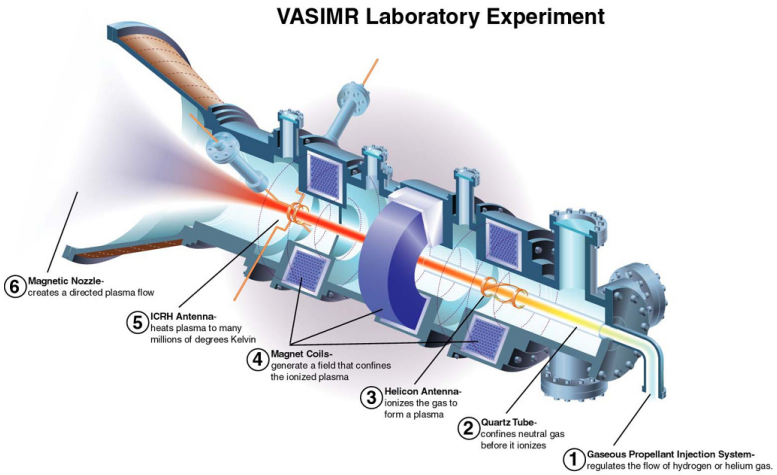

Figure 1.1: A schematic drawing of the VASIMR VX-10 prototype.[6]

experimental effort focused on exhaust plume diagnostics for characterizing plasma detachment from a magnetic nozzle. Plasma detachment is the process whereby the exhaust trajectory of the propellant plasma diverges from the magnetic field lines in a vacuum. In the classical Magnetohydrodynamic theory of magnetic plasma confinement the constituent ions and electrons are constrained to move only along the magnetic field lines and not across them. Plasma detachment is important to the VASIMR technology because all magnetic field lines are ultimately closed so the propellant must eventually detach from the magnetic field lines in order for the engine to generate thrust. The effective nozzle efficiency of the VASIMR engine can be calculated by determining at what point in the expanding exhaust plume the ideal Magnetohydrodynamic scenario breaks down.

The plasma detachment experimental arrangement consisted of a small pulsed plasma source in a large vacuum chamber. The plasma source was a washer stack plasma gun constructed at the University of Washington. Current carrying coils mounted on the outside of the vacuum chamber provided the guiding magnetic field. The chamber contained a

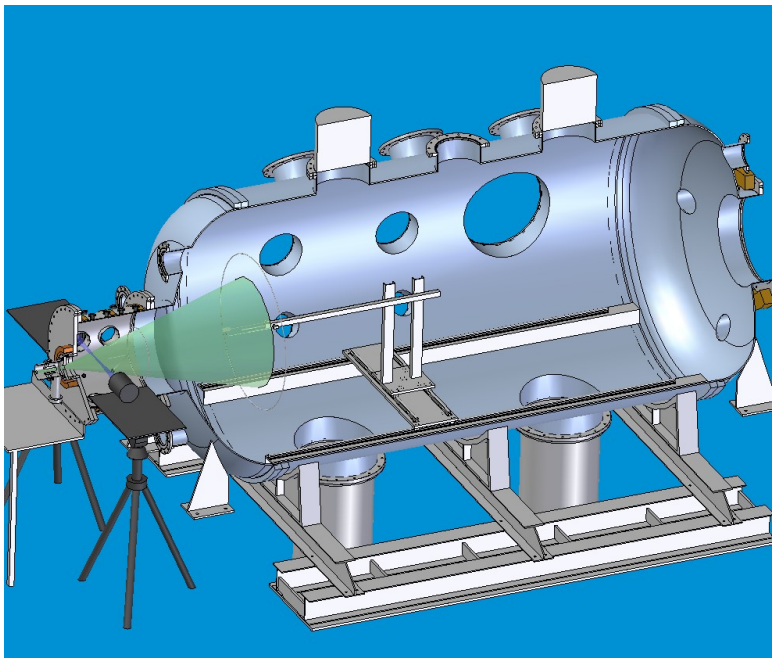

Figure 1.2: Schematic drawing of the DDEX facility.

translation stage with two degrees of freedom. Diagnostics packages including Langmuir probes, for measuring the plasma density, and Hall effect magnetic sensors were mounted to the translation stage. The Bdot loops described in this thesis were also mounted to the translation stage. Figure 1.2 is a three dimensional rendering of the DDEX setup showing the plasma source, predicted exhaust cone, translation stage and large vacuum chamber.

For a study of magnetic detachment phenomenon it is important to map the nozzle magnetic field in vacuum. This determines the shape of the nozzle. The magnetic field due to a set of current carrying coils can, of course, be calculated. But it is important to be able to compare that calculation to experimental data. For this purpose a three dimensional Hall probe sensor was developed for the DDEX project. It is equally important to know how the magnetic field changes when plasma is created. Those changes will be over a very short

timescale, too short for the Hall probes to detect. The purpose of this thesis is to explore the spatial and temporal structure of this disturbance in the magnetic field with Bdot probes capable of detecting high frequency (MHz) oscillations. Bdot probes measure changes in magnetic flux rather than steady state magnetic field strength. For this reason they are the preferred measurement method for observing changes imposed by the propellant plasma on the vaccuum magnetic field structure.

Because the plasma detachment process has still not been experimentally verified it is not yet clear how accurately the current analytical and numerical models predict the actual nozzle efficiency. Additional magnet coils may be necessary to increase the efficiency of the magnetic nozzle. These nozzle coils could substantially increase the total mass and cost of the cryogenic superconducting magnet system. But the necessity and geometry of such coils is intimately connected with the plasma detachment process. The proposed MHD scenario[8] requires an extended nozzle field to ensure efficient plasma detachment. However, high frequency instabilities in the plasma may violate the frozen-in ideal MHD model of plasma detachment.[9] In reality, plasma detachment will probably be due to a combination of field dragging and anomalous diffusion. Simulations of plasma detachment[10] have indicated that additional nozzle coils are a worthwhile investment, but insufficient experimental evidence has been gathered to date to show that the long magnetic nozzle field generated by additional superconducting coils is neccessary for optimal rocket performance. The research presented here is expected to clarify the dominant detachment mechanism in a magnetic nozzle configuration by indicating to what extent the propellant plasma influences the magnetic field geometry in the exhaust plume.

Chapter 2

Magnetic Nozzle Theory

The primary purpose of the magnetic nozzle section of the VASIMR engine is to convert the ion energy into a directed flow.[8] Power is deposited in the ions by radio waves whose frequency matches the natural ion cyclotron frequency of the propellant ions in the confining magnetic field. The absorption of these waves increases the ions' velocity perpendicular to the magnetic field. In plasma physics a distinction is often made between temperature or particle kinetic energy perpendicular and parallel to the magnetic field. Ion Cyclotron Heating increases particle kinetic energy perpendicular to the magnetic field. In other words it increases $v_\perp$. The magnetic nozzle concept makes use of the conservation of the magnetic moment of a charged particle, often referred to as the first adiabatic invariant.[11] The magnetic moment of a gyrating charged particle, which is typically denoted by the greek letter μ but is unrelated to the magnetic permeability, is a constant of the motion. The magnetic moment is defined as the ratio of perpendicular kinetic energy to magnetic field strength. Perpendicular kinetic energy is related to the component of the ion velocity perpendicular to the magnetic field direction.

$$\mu = \frac{\frac{1}{2}mv_\perp^2}{B} \tag{2.1}$$

From this we can see that as the magnetic field strength diminishes in the magnetic nozzle, the perpendicular velocity of the ions must also diminish. Since the total kinetic energy of the ions is conserved, this leads to an increase in the velocity parallel to the magnetic field. In this way the ions are accelerated in the axial direction.

This particle acceleration process can also be viewed as simply the conservation of angular momentum. As the magnetic field diminishes, the gyroradius of the charged particles increases. The gyroradius, or Larmor radius, of a charged particle in a magnetic field is given by equation 2.2.[12]

$$r = \frac{mv_\perp}{qB} \tag{2.2}$$

Since the angular momentum $L = mrv_\perp$ must remain constant, the perpendicular velocity must decrease as the gyroradius increases. A particle's gyroradius is inversely proportional to the magnetic field strength. A particle's angular momentum is proportional to the square of the perpendicular velocity and inversely proportional to the magnetic field strength.

$$L = \frac{m^2 v_\perp^2}{qB} \tag{2.3}$$

So as the magnetic field strength decreases the velocity perpendicular to the magnetic field vector must also decrease. Again conservation of energy decrees that if the perpendicular velocity decreases then the parallel velocity must increase and so the ions are accelerated parallel to the magnetic field.

Both of these explanations of particle acceleration in a diverging magnetic nozzle field are from the viewpoint of a moving particle in a stationary magnetic field. An alternative description of the acceleration process is to treat the field generating coils and the particles as two separate magnetic elements. The rotation of the charged particle in the magnetic field will be opposite to the currents in the coils and there will therefore be a repulsive force

between the two. This leads to an acceleration of the particle with respect to the coil and an equal and opposite force on the magnetic coil.

After the magnetic nozzle has accelerated the ions in the axial direction the ions must detach from the magnetic field. If they continued to follow the closed magnetic field lines they would eventually impact the spacecraft. These ions would cause damage to the space craft and not contribute to engine thrust. It is well known in the field of space physics that it is possible for energetic ions to escape from confining magnetic fields. Sometimes this happens with violent results, such as solar flares. But the process responsible for detachment in the VASIMR technology is still unclear. There are several ways to look at the problem. Any of the following conditions can be viewed as a defining criteria for exhaust plasma detachment.

1. Plasma energy density exceeds magnetic field energy density.
2. Exhaust flow velocity exceeds Alfvén speed.[8]
3. Ion orbits exceed magnetic field dimensions.[10,13]

The Alfvén speed is the speed at which magnetic disturbances travel in a plasma. Its influence is analogous to that of the sound speed in a chemical rocket. After the flow velocity of the propellant has exceeded the Alfvén speed events downstream of that point in the exhaust cannot affect events upstream. This is equivalent to choked flow in a de Laval nozzle. The Alfvén speed is defined as[14]

$$v_A = \frac{B}{\sqrt{\mu_0 \rho}} \tag{2.4}$$

Where μ_0 is the permeability of free space and ρ is the mass density of the plasma.

It will be shown here that the first two conditions for detachment are identical. The ratio of plasma energy density to magnetic field energy density is often used in the study of magnetically contained plasmas. This ratio is conventionally labeled β.[11]

$$\beta = \frac{2\mu_0 nkT}{B^2} \tag{2.5}$$

In this case we will use the energy density of the directed flow of the plasma, which is a function of ion velocity v, rather than the plasma pressure, which is a function of ion temperature T.

$$\beta = \frac{\mu_0 \rho v^2}{B^2} \tag{2.6}$$

When this directed flow energy density becomes greater than the magnetic pressure ($\beta > 1$) then the momentum of the exhaust overcomes the guiding force of the magnetic field. This is equivalent to condition 1 above. It is easy to show that the conditions $\beta > 1$ and $v > v_A$ (which is condition 2 above) are the same. The author is not aware of this development occuring in any previous publications.

$$\beta > 1 \Rightarrow \frac{\mu_0 \rho v^2}{B^2} > 1 \Rightarrow v^2 > \frac{B^2}{\mu_0 \rho} \Rightarrow v > \frac{B}{\sqrt{\mu_0 \rho}} \Rightarrow v > v_A \tag{2.7}$$

Evaluation of the third possible defining criteria for plasma detachment, where the ion Larmor radius exceeds the magnetic field curvature, requires a discrete particle analysis in a specified confining field geometry. This analysis would be outside the scope of the present research, but is mentioned here for completeness. The interested reader is directed to the references[10,13] for an example of a numerical simulation of this case. The ions in the exhaust

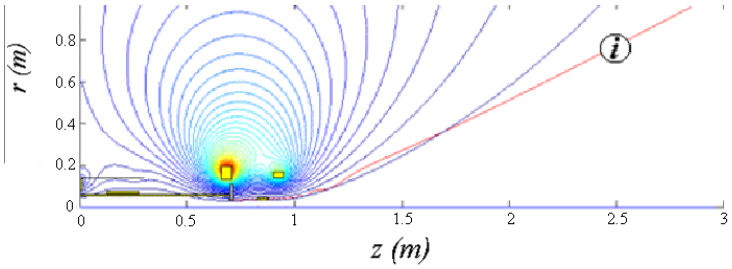

Figure 2.1: Single particle trajectory calculation for an ion exiting the VASIMR engine.[10]

would very quickly deviate from the magnetic field if they were on their own, as is evident from the ion orbit calculations reproduced in figure 2.1. However it is important to realize that the exhaust is quasineutral, or composed of equal numbers of ions and electrons. Single particle calculations for an electron show that the electrons have a much smaller Larmor radius in the magnetic field and are more tightly bound to it. Since the ions carry the majority of the momentum in the exhaust and the electron and ion motions are bound by their mutual attractions through electric field interactions the electrons must eventually be pulled along with the ions. This can happen through either cross field diffusion of the electrons or magnetic field dragging by the exhaust plasma. The current driven instability postulated by researchers at KTH[9] indicates an anomalously fast cross field diffusion rate, whereas the magnetohydrodynamic scenario advanced by researchers at the University of Texas[8] describes a situation in which the magnetic field is frozen into the exhaust flow.

Each of the three conditions outlined above involves a relationship between the exhaust plasma and the confining magnetic field. Plasma entering the magnetic nozzle region is well confined by the magnetic field, but this quality changes over the spatial dimensions of the plume. There is a simple argument which demonstrates that the conditions for plasma detachment are present in an expanding magnetic nozzle configuration. If the plasma acts

as an ideal magnetohydrodynamic fluid then the total magnetic flux in the exhaust plume is conserved. The magnetic field is "frozen in" to the plasma. This means that the magnetic field strength (or flux density) is inversely related to the cross sectional area as the plume expands in the axial direction. Using r_p to represent the plasma radius, this means

$$B \propto r_p^{-2} \tag{2.8}$$

Because the total particle flux is also conserved, the number density will also vary inversely with the cross sectional area. This is strictly true only if the axial particle velocity is constant, so the nozzle region under consideration here is the section after the majority of the axial particle acceleration has already occured.

$$n \propto r_p^{-2} \tag{2.9}$$

The magnetic pressure (or magnetic field energy density) is proportional to the square of the magnetic field strength.[11] All these factors combine to imply that the magnetic pressure will drop faster than the particle energy density as the plume radius expands. In fact because the ion kinetic energy (W) is conserved in the expansion region the ratio of plasma energy density to magnetic pressure (β) is proportional to the plume area.

$$\beta \propto \frac{nW}{B^2} \propto B^{-1} \propto r_p^2 \tag{2.10}$$

This is illustrated graphically in Figure 2.2.

There is yet another process which will lead to particle detachment and that is the recombination of the ions and electrons in the exhaust plasma. Once this recombination

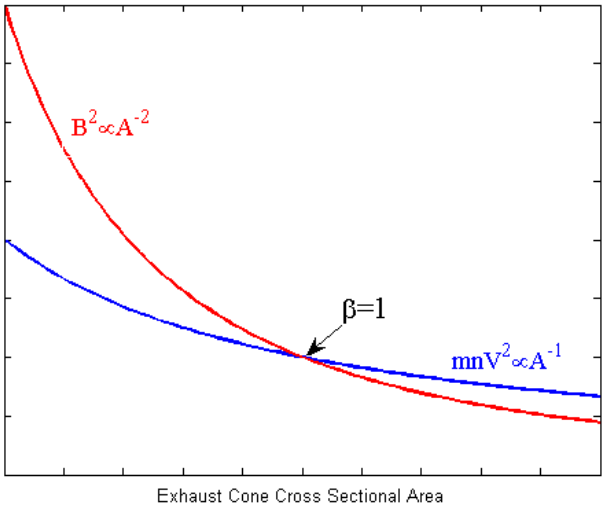

Figure 2.2: A graphical comparison of the evolution of particle and magnetic field energy density in an expanding magnetic nozzle.

takes place the neutral atoms are no longer affected by the guiding magnetic field. Unlike the typical ion engine which accelerates propellant ions separately from electrons the VASIMR concept retains a quasineutral plasma throughout the acceleration process, which means that there are no space charge limitations on the design. Because of this there is no need to provide an electron emitter after the ion acceleration section as in the standard ion engine design. No serious attempt has been made to either predict or measure the recombination rate in the exhaust plasma. The quick rise in background neutral pressure inside the vacuum chamber during a plasma firing is the chief experimental difficulty to be overcome in measuring magnetic nozzle detachment phenomena. This effect is particularly prominent in charge exchange collisions and makes the issue of recombination rate confusing. Limitations on available chamber volume and pumping capacity mandate very short plasma pulses. Estimates of the recombination rate could be made based on the plasma density and electron

and ion temperatures in the exhaust region, but it is believed that the recombination rates will be low enough to not play a significant role in the evolution of the exhaust plume.

As with any rocket system, there will be some divergence of the exhaust flow from the desired thrust direction. This results in an effective nozzle efficiency which is due to the half-angle of the exhaust cone it forms. In the case of a magnetic nozzle the half angle is determined by the magnetic field direction at the point in the plume where the plasma flow begins to deviate from the vacuum magnetic field lines. The outer parts of the plasma will be diverted from total axial flow before the plasma becomes sufficiently detached from the magnetic field. If we assume that the density and velocity of the exhaust plasma are uniform over the cross section of the exhaust plume, then the equation for nozzle efficiency is the same as that for a chemical rocket nozzle.

$$\eta = \frac{1 + \cos\theta}{2} \tag{2.11}$$

Where θ is the half angle of the nozzle. The dipole magnetic field from a single current carrying coil diverges rapidly from the axial direction. It has been suggested[8] that additional current carrying coils may be necessary to increase the efficiency of the magnetic nozzle configuration. Such coils would force the vacuum magnetic field to expand more slowly in the nozzle region, thus lowering the field strength to below the level necessary for plasma detachment while maintaining the flow directivity needed for efficient nozzle operation. However, the extent to which the presence of the plasma itself modifies the vacuum magnetic field generated by the plasma confining magnetic coils has not yet been experimentally determined.

In order to analyze the magnetic field perturbations observed in DDEX it will be useful to compare the data with analytical predictions. The model used here will be that of Ilin et al.[10]

$$\frac{B_p}{B} = \beta \frac{r_p}{a_p} \tag{2.12}$$

Where B_p is the magnetic field inside the plasma, B is the vacuum field generated by the magnetic coils alone, r_p is the plasma radius and a_p is the magnetic field curvature.

Figure 2.3 displays the results of two different numerical simulations of exhaust plasma detachment from the VASIMR thruster.[10] These simulations illustrate the amount of divergence from the axial direction that is expected from current theoretical and numerical models of the exhaust plume. The correlation between the two different techniques of numerical modeling, both ideal magnetohydrodynamics and discrete particle analysis, reinforce the conclusion that detachment will occur in the device. The results of these simulations agreed well with the analytical predictive formula of Equation 2.12.

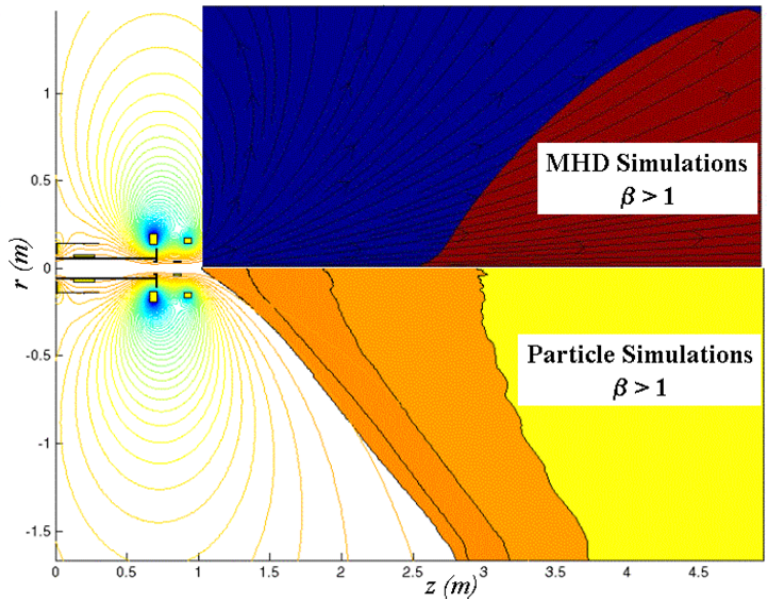

Figure 2.3: Exhaust plume of the VASIMR thruster predicted from MHD simulations.[10]

Chapter 3

Magnetic Probe Calibration

A Bdot probe constructed by collaborators at the Alfvén Lab in Stockholm was brought to the Marshall Space Flight Center to search for evidence of magnetic field bending and plasma detachment in the magnetic nozzle configuration. The Bdot probe is a simple, passive device for measuring time varying magnetic fields.[15] Bdot probes consist of a loop or coil of wire, the leads of which are connected to a voltage recording instrument or digitizer. The operating principle of a Bdot probe is Faraday's Law of Electromagnetic Induction. A changing magetic flux through the loop will induce an emf across the leads.[12]

$$\mathcal{E} = -\frac{d\Phi}{dt} \tag{3.1}$$

Figure 3.1 illustrates the basic design of a Bdot probe. The probe response is dictated by the number of turns in the coil and the area of the coil. The probe area includes any area between the lead wires which attach the loop to the voltage recording instrumentation. The leads of the probe are usually twisted together to offset this effect.

If the probe loop is small enough in diameter then the assumption can be made that the magnetic field is the same over the area of the loop and the total magnetic flux through the loop is simply the magnetic field strength perpendicular to the loop multiplied by the loop area multiplied by the number of turns the loop is comprised of. If the loop diameter and number of turns are known then the relative variation in magnetic field strength can be calculated by integrating the recorded voltage over the time period of interest.

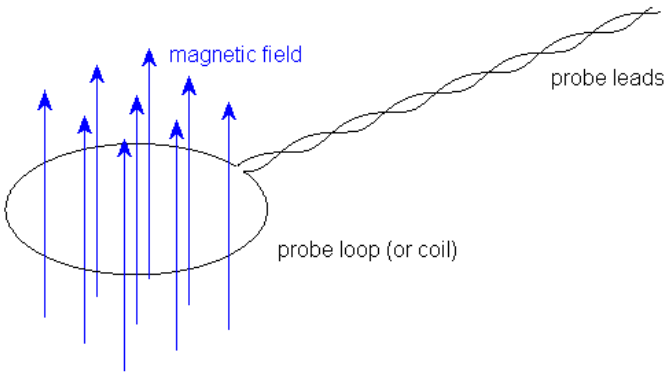

Figure 3.1: Diagram of Bdot probe operating principle.

The Bdot loops used in this research were originally constructed for measuring high frequency fields in the related VX-50 experiment at Johnson Space Center. These electromagnetic field probes were constructed at the Alfvén Laboratory of the Royal Institute of Technology (KTH) in Stockholm, Sweden. They consisted of three mutually orthogonal single loops of wire. The loops were 5mm in diameter. A mount was fabricated at the Propulsion Research Center for attaching a probe to the translation stage in the Detachment Demonstration Experiment. A schematic drawing of the probe mounting is presented in Figure 3.2. This figure also indicates the polarity of the Bdot loops with respect to the vacuum chamber coordinate system. Increasing magnetic field strength in the direction indicated in the Figure produced a positive voltage at the digitizer.

The photograph in Figure 3.3 was taken from the perspective of the translation stage inside the vacuum chamber. The perspective of the picture is looking "upstream" towards the plasma source and the plasma gun in the end of the narrower cylindrical vacuum chamber

section beyond the large flux loop can be seen at the top of the image. The Bdot probe is mounted on the translation stage arm and sticks out horizontally to the right. There is a triple Langmuir probe sticking vertically up from the end of the translation stage arm. The coaxial signal cables are also visible coming from the bottom of the probe mount and going inside the hollow aluminum box beam of the translation stage arm.

The probe also incorporated two sets of electric field probe tips. The data from those probe components was recorded during the experimental pulses. The data from the B_ϕ loop was not recorded because of lack of feed throughs for the signal cables. There were five components in the probe, three Bdot loops and two sets of electric field probe tips. Only four coaxial signal feedthrus were available on the vacuum chamber, so the B_ϕ component was disregarded because the geometry of the experiment is azimuthally symmetrical so no variation in the ϕ direction was expected. The original purpose of the Bdot probe was to detect high frequency excitations. Such excitations are conjectured to be the result of a plasma instability that could cause unusually fast diffusion of the plasma across the magnetic field lines.[9] This phenomena could potentially result in much more efficient nozzle detachment than would be expected from the ideal MHD detachment model. Unfortunately no high frequency components were observed in the data collected and presented here.

Signal lines were constructed of 50Ω coaxial cable. Inside the vacuum chamber the coaxial cable was RG-188 fluoropolymer insulated type. The signal lines ran through BNC vacuum feed throughs into standard RG-58 coaxial cable and from there to the digitizer equipment. The complete signal path was tested with a network analyzer after installation before closing the vacuum chamber. The signal path showed a completely linear phase response and negligible attenuation. This test is an important part of the experimental

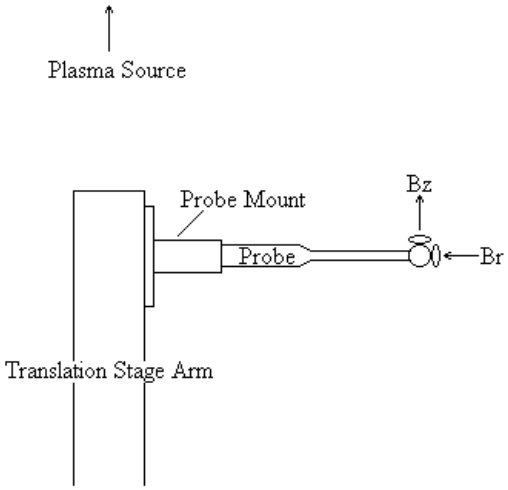

Figure 3.2: Diagram depicting the mounting of the probe on the translation stage and the polarity of the loops viewed from above.

setup because it shows that, had any high frequency instabilities been present, they would have been observable in the recorded data.

The Bdot probe was calibrated in the following way. The entire calibration configuration (pictured in Figure 3.4) was taken inside the chamber. Clockwise from the left in that picture are the Helmholtz coil for producing the calibration magnetic field (labeled 1.243Gauss/Amp), Pearson coil for measuring the current through the Helmholtz coil, Tektronics digital oscilloscope for recording the current waveform and a current pulser for energizing the Helmholtz coil. The items resided just inside the vacuum chamber for this picture. One of the large diffusion pump ports is visible in the background, as well as the back edge of the translation stage. The Helmholtz coil was held up to the probe and a pulse of current was sent through the coils with the current pulser. The current through the Helmholtz coil also ran through the Pearson current transformer (model 301X) which was labeled "0.01 Volts per Amp." The output of the current transformer was recorded by

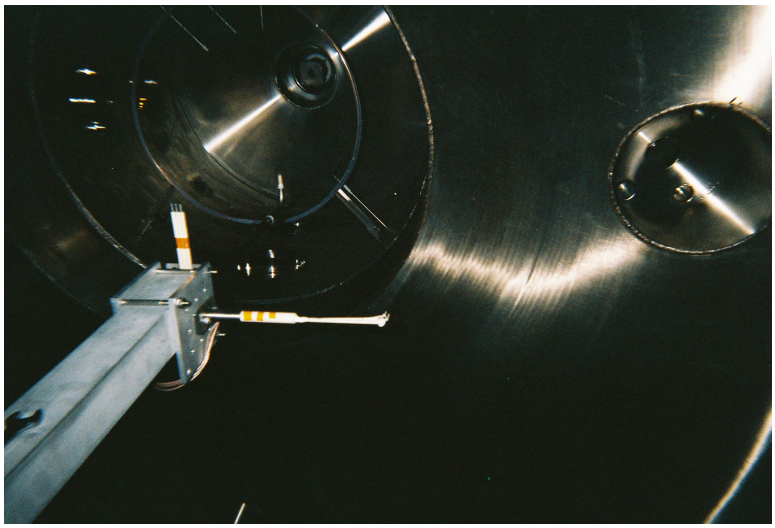

Figure 3.3: Photograph of Bdot probe mounted on translation stage arm.

the Tektronix TDS 3052 oscilloscope. The data from those voltage waveforms was written to Excel™Spreadsheet files. This data was later read into Matlab®for calculations. Figure 3.5 displays the calibration magnetic field generated by the Helmholtz coils. This is determined by multiplying the voltage data recorded by the oscilloscope by the calibration markings on the Pearson current meter and the Helmholtz coil. Figure 3.6 displays the voltage output from a Bdot loop which was recorded by the digitizing module for the calibration pulse. This data must be integrated to obtain the magnetic field strength as a function of time.

The voltage output of the Bdot probe (displayed in Figure 3.6) must be numerically integrated with respect to time over the calibration pulse period in order to retrieve the change in magnetic field strength. This is because the voltage across the probe leads is proportional to the time rate of change in magnetic flux. A linear slope is introduced by integrating the data and is obvious in Figure 3.7. The linear slope is caused by the random voltage offset of the digitizer. This can be effectively eliminated by subtracting an offset

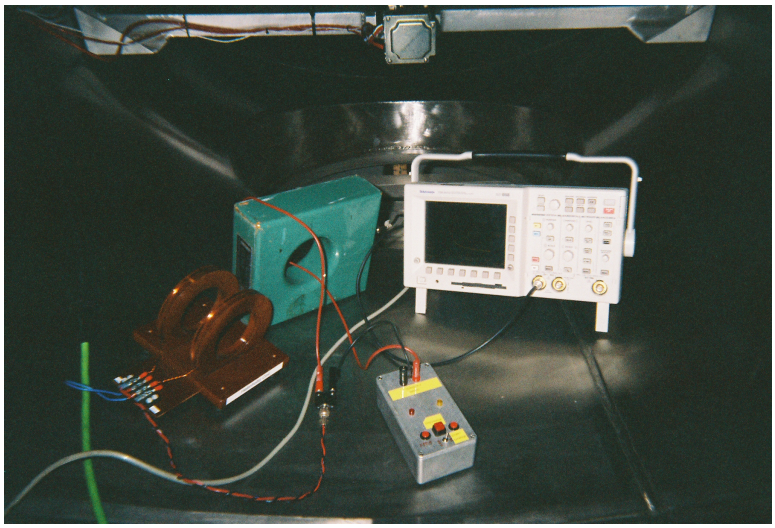

Figure 3.4: Equipment used for calibrating the Bdot probes.

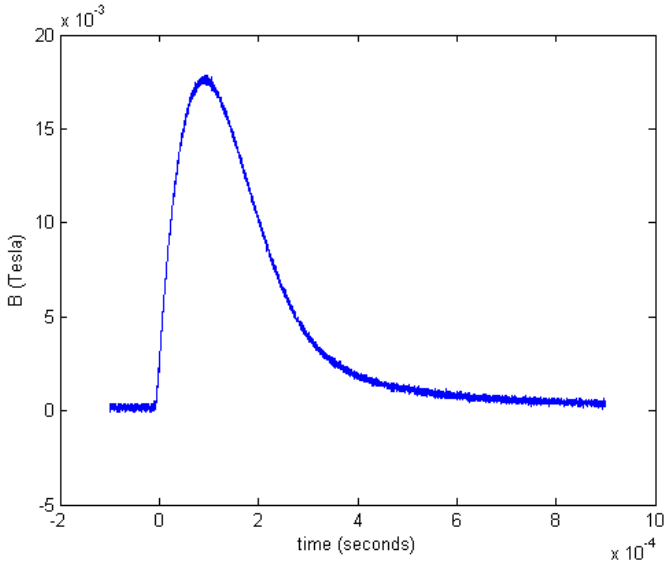

Figure 3.5: Magnetic field strength produced by the Helmholtz coil during the calibration pulse.

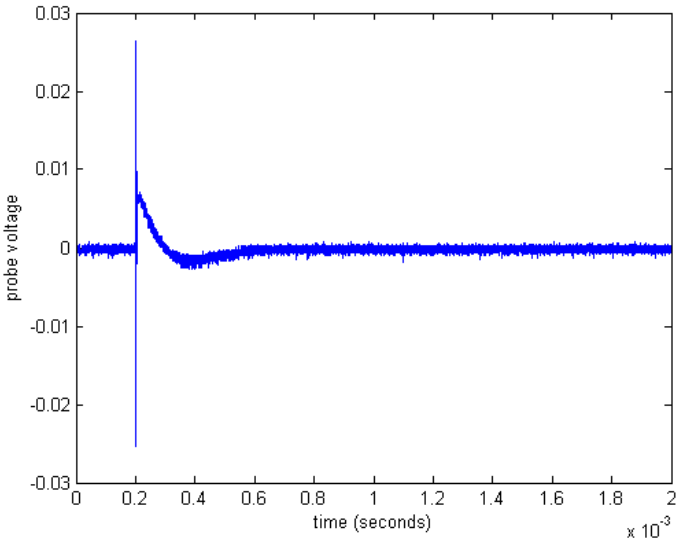

Figure 3.6: Raw voltage data from the Bdot probe recorded by the digitizer.

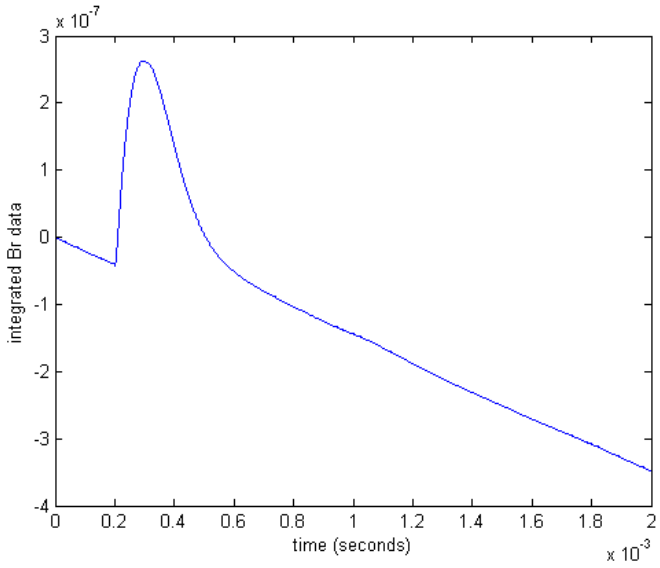

Figure 3.7: Results of numerically integrating the probe voltage displayed in figure 3.6

voltage from all points in the data set. A simple way of determining the offset voltage is to average over some time period when the voltage should be zero. During calibration and subsequent data analysis the first 0.2ms of points before the pulse were averaged to determine the offset to subtract. After this is done the voltage should be scaled according to the area of the Bdot loops (A) and the number of turns (n). This nA calibration term is the parameter of interest and was determined by analyzing data from the calibration pulses. The Swedish collaborators who manufactured these probes made the loops to be 5mm in diameter. The initial assumption was that each loop was a single turn. After analyzing the data from the calibration pulses it was realized that this was not a good assumption. The conclusion reached from the calibration data analysis was that the Br loop consists of one turn and the Bz loop is two turns. So the calibration factors should be $nA = 1.96 \times 10^{-5}\text{m}^2$ for the Br loop and $nA = 3.92 \times 10^{-5}\text{m}^2$ for the Bz loop. Figures 3.6 and 3.7 are plots of the calibration magnetic field and the integrated probe data for both the Br calibration pulse and the Bz calibration pulse. Note that in Figure 3.8 there is some response of the Bz loop to magnetic field in the r direction and vice-versa in Figure 3.9. This is because the magnetic axes of the Br and Bz loops are not entirely orthogonal. In particular, the Bz loop is more sensitive to changes in Br than the Br loop is to changes in Bz. This is to be expected since the Bz loop is actually composed of two turns.

An interesting behavior can be observed in the calibration data plot Figures 3.8 and 3.9. The magnetic field produced by the Helmholtz coil obviously drops to zero after the current pulse is finished. But the integrated voltage data from the Bdot probe never completely drops back to zero. This can be explained as an artifact of the numerical integration procedure combined with the probe sensitivity and digitizer response. The number of turns

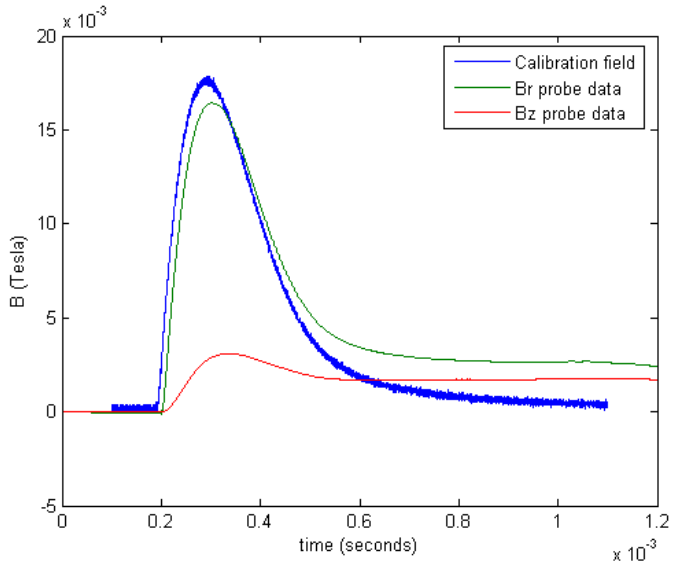

Figure 3.8: Magnetic field and probe response for Br calibration pulse.

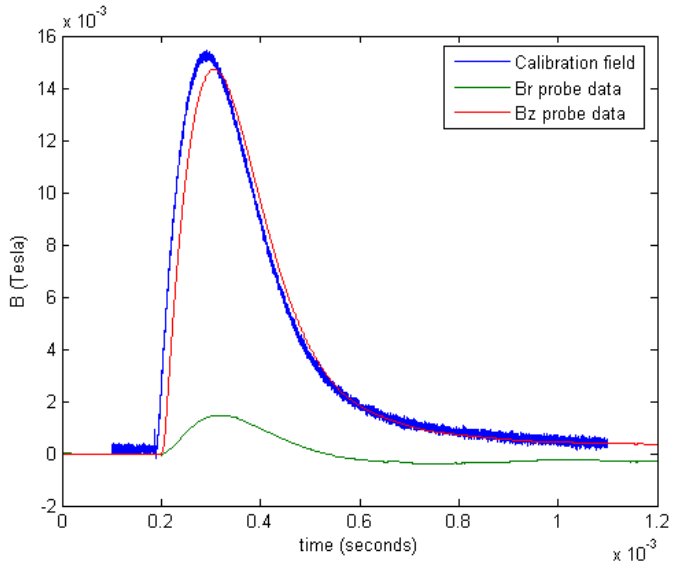

Figure 3.9: Magnetic field and probe response for Bz calibration pulse.

in the probe coil was intentionally made small to leave the probe receptive to high frequency variations in magnetic field strength. A large number of turns increases the self inductance of a coil which effectively damps high frequency oscillations.[16] The small number of turns means that the probe has a small response or low gain. Since the voltage output of a Bdot probe is proportional to the time rate of change of the magnetic field strength, a slowly decaying magnetic field produces a smaller output voltage than a quickly changing one. As the magnetic field produced by the Helmholtz calibration coil asymptotically approaches zero after the current pulse the voltage data from the Bdot probe becomes too small to see over the random offset of the digitizer equipment. The offset subtraction and numerical integration procedure then produces a profile of magnetic field strength that seems to never return to the pre-pulse value.

In order to increase the probe response but still keep the small spatial resolution the number of turns in the loop could be increased to increase the effective area. One negative effect of this technique is that increasing the number of turns increases the skewing of the magnetic axis of the probe. Increasing the number of turns has the effect of adding some probe area in a different direction than the direction intended. Notice in the calibration graphs (Figures 3.8 and 3.9) that while the double loop Bz seems slightly more responsive to the Bz calibration pulse, it is also more responsive to the Br calibration pulse. Increasing the number of turns in the loop also has the effect of increasing the self inductance of the probes. This generally lowers the probe responsiveness to higher frequency magnetic field oscillations.[16]

Chapter 4

Plasma Density Measurements

One of the key components of the diagnostic efforts on the DDEX project was determining the plasma number density in the exhaust cone. Examining the spatial evolution of the propellant plasma as it travels through the expansion region is an important step in understanding the detachment process. Two separate measurement techniques formed the basis of this diagnostic system. These were a multiple frequency microwave interferometer system[17] and a pair of triple langmuir probes that were mounted on the internal translation stage. The operating principles of both the microwave interferometer and the langmuir probe are covered in detail in the excellent text by Hutchinson.[15] The microwave interferometer system provides a good absolute measurement of electron number density in the plasma integrated along the line of sight. The system was located at z=0.4m on the DDEX vacuum chamber and situated to look directly across the plume. The data from the microwave interferometer system provides an excellent record of the total amount of plasma created by the washer stack plasma gun, but does not give detailed information on the radial distribution of that plasma. The triple langmuir probe serves to measure the electron density with a very good spatial resolution. Because of its mounting point on the internal translation stage this probe can be moved across the exhaust cone to provide a profile of plasma density. However the pulsed nature of the experiment means that a scan must be performed over multiple shots. The variations in propellant plasma created by the washer stack gun from shot to shot make the triple probe data alone difficult to interpret. It is necessary to separate shot to shot variations in plasma density from spatial variations and

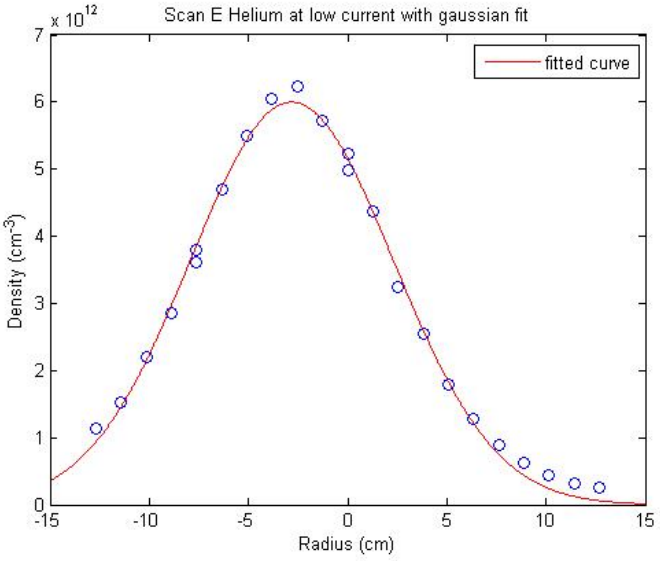

Figure 4.1: Radial profile of plasma density at z=43cm in the DDEX exhaust plume.[18]

for this purpose it is useful to employ the microwave interferometer system as an indicator of overall plasma source performance. In this role the density measured by the triple probe over the course of several pulses which comprise a radial scan is rescaled by multiplying by a scaling factor obtained from the interferometer data. The scaling factor for a particular shot is obtained by dividing the line integrated electron density for that shot by the average value for the set of shots. The results of such a data analysis algorithm are displayed in Figure 4.1 for a radial scan. The discrete points are langmuir probe data points rescaled by interferometer results. The line is a Gaussian fit to the density profile. This radial density profile will be useful for comparison with the magnetic field perturbation measurements presented in the next chapter.

Chapter 5

Magnetic Field Measurements

After the Bdot loops were calibrated the vaccuum chamber was sealed and pumped down. Bdot probe data was recorded during each pulse of the plasma source. The translation stage position was changed between shots to allow a radial mapping of the magnetic field data. Data from the Bdot loops was numerically integrated to determine a ΔB during the plasma shot.

An initial high frequency signal component is obviously present in the raw probe voltage data. Numerical integration of the data yields unexpected results. As previously noted the offset of the digitizer results in a linear plot of some random slope when the signal is integrated. This slope changes from one shot to the next without any apparent pattern. This effect is accounted for in the analysis of the data by subtracting an offset voltage from the raw data before integration.

The initial ΔB signal upon integration produces a jump or discontinuity in the linear plot caused by the digitizer offset. This can be seen in Figures 5.1 and 5.2. Several interesting phenomenon can be observed here. If the plasma drags the magnetic field lines with it as is theoretically predicted then the magnetic field profile should return to its vacuum state after the plasma disappears. This is not observed in the experiment. What is observed is a sudden change in the magnetic field strength, but no clear, complete change back to the original. One possible explanation for this is that the plasma appears quite suddenly when it is produced by the washer stack plasma gun, but diffuses out into the chamber over a longer time scale. Therefore the initial change in magnetic field should occur quickly, but

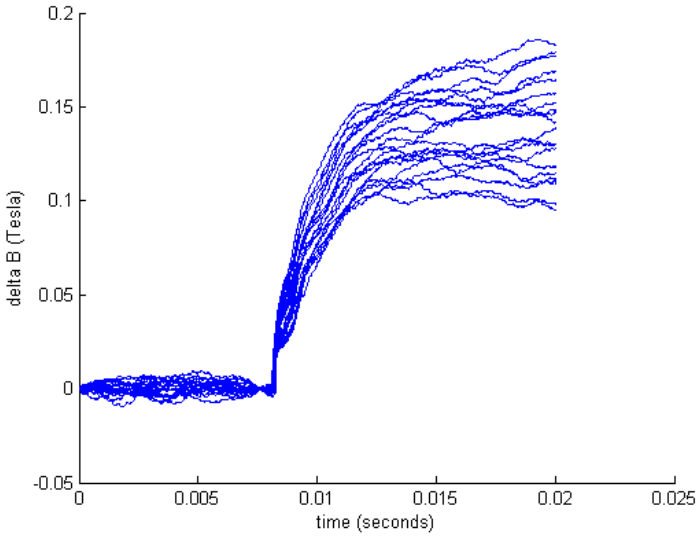

Figure 5.1: ΔB_r data from twenty consecutive shots on machine axis.

the decay back to the original state will take longer. Since the voltage produced by a Bdot loop is directly proportional to the rate of change of the magnetic field it is possible that the decay back to the original magnetic configuration does not produce a large enough probe voltage to be observable.

An attempt was made to record data for a longer period of time after the plasma pulse by lowering the digitizer sampling rate. Since the voltage recording equipment allowed for a finite number of samples a trade off had to be made between temporal resolution and total data recording time. So for example one could record 20ms of data at 500kHz or 1s of data at 100kHz. However, no evidence was found for a return of the magnetic field strength to the vacuum conditions, no matter how long data was recorded.

Another interesting effect is that the slope of the straight line caused by integrating the digitizer offset sometimes changes after the shot. It's almost as if the small ΔB signal that is present at the beginning of the shot changes the electronics of the digitizer. One

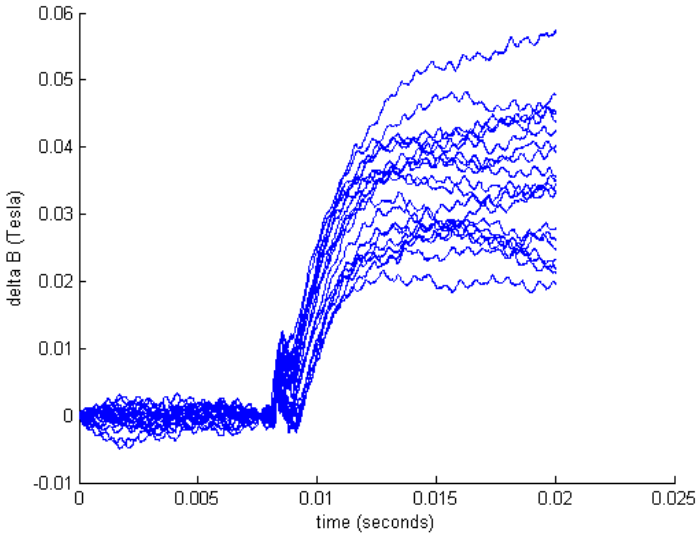

Figure 5.2: ΔB_z data from twenty consecutive shots on machine axis.

outcome of all of this is that it is obvious now that numerically integrating the digitized signal from a Bdot probe is not the best technique for finding the net change in magnetic field strength. An attempt was made at using a passive RC integration circuit between the probe and the digitizer. This would integrate the Bdot probe signal before it reaches the digitizer and obviate the need for a numerical integration of the digitized voltage data. But this architecture was unproductive since the passive integrator circuit also decreases the signal strength at the digitizer. Future attempts at measuring the changing magnetic field would do well to incorporate an active op-amp integration circuit between the probe and the digitizing hardware.

In doing the radial probe scans the implicit assumption is made that the plasma conditions do not vary from shot to shot. This is not a very good assumption because the pulsed plasma gun used as a source in this experiment produces variable discharges. Figures 5.1 and 5.2 are a good characterization of the variability of the magnetic field perturbations

over a range of experiment pulses. Relying on the repeatability of the data from shot to shot is not a good technique for measuring spatial profiles of plasma properties in the exhaust plume. An alternative technique would include constructing a multiple loop probe that could simultaneously measure disturbances at several locations. However, increasing the physical dimensions of the probe raises questions about the perturbation of the tenuous plasma stream by the measuring instrument. An attempt was made to quantify the variability of the recorded data by firing multiple plasma pulses while leaving the translation stage in a fixed position. The results of twenty consecutive pulses taken with the probe on machine axis are presented in Figures 5.1 and 5.2. The variability in ΔB observed in these shots is used to assign error bars to the radial profile plots in Figures 5.5 and 5.7. This was done by calculating the standard deviation of the change in magnetic field strength in both the radial and axial direction for the twenty consecutive shots on machine axis. The errorbars included in Figures 5.5 and 5.7 reflect a 2σ uncertainty in the measured ΔB based on the sequence of measurements on machine axis.[19] Multiple shots were not taken at every radial location due to time constraints. The limited machine time devoted to this particular investigation coupled with the charging time of the firing capacitor did not allow for multiple plasma pulses at every point in the scan.

Figure 5.3 displays a cross section of the DDEX vacuum chamber along with the calculated magnetic field lines created by the magnet coils. The downward curve in the field lines as they enter the main chamber is a result of the ambient magnetic field of the earth. The strength of the artificially generated field begins to fall below the earth's naturally occuring magnetic field strength as the plasma travels farther from the field generating coils. Therefore the magnetic field line orientation in the main chamber is determined predominantly

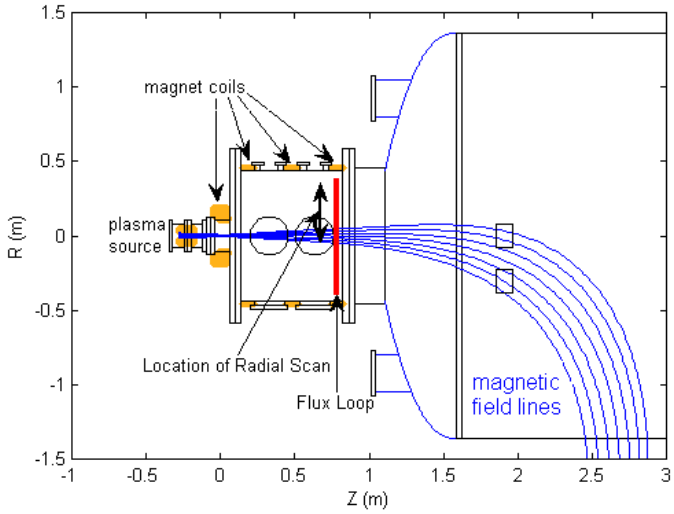

Figure 5.3: Calculated magnetic field lines in the DDEX machine. The location of the radial Bdot probe scan is indicated with a black double arrow.

by the direction of the earth's magnetic field in Huntsville Alabama. These are the field lines that should be present under vacuum conditions. The presence of a plasma inside the chamber will alter this magnetic field topology. The goal of this research is to investigate to what extent the vacuum fields are altered by the plasma.

It was found that the change in magnetic field strength recorded by the Bdot loops varied as they were moved radially across the plume. The radial scan took place at an axial location of z=0.633 meters in the nozzle coordinate system. This location is indicated in Figure 5.3. The data obtained during a sequence of plasma pulses comprising a radial scan of the plume is presented in Figures 5.4 and 5.6. The polarity of the data was reversed during the analysis process so that the coordinate system would coincide with the magnetic nozzle system. This is more sensible than the probe coordinate system indicated in Figure 3.2 which was determined by the probe mounting orientation.

The digitized voltage signal from the Bdot probe was numerically integrated after the digitizer offset was subtracted out. The result was multiplied by the calibration factors previously obtained. Figure 5.4 shows the axial magnetic field data from a radial scan comprised of shots 12 thru 31 from February 24th 2006. The translation stage position was moved 1 inch between each pulse. This plot demonstrates another interesting characteristic of the discharge. For the first 4 shots (r=0 to 4 inches from machine axis) the plotted data is rather smooth. Thereafter some additional sinusoidal component appears in the data. It is unknown why this would be the case. It might be due to some instability in the plasma at the edges of the discharge. But more likely it is because the plasma discharge from the washer stack plasma gun is not very reproducible. From this data ΔB_z can be plotted as a function of radial position in the plume. This was done in Figure 5.5. The same radial profile analysis was done for the radial component of the magnetic field and is presented in Figures 5.6 and 5.7.

There were two large Bdot loops, referred to as flux loops, which encircled the entire plasma column. The integrated ΔB profile measured by the small Bdot loops can be compared with the total change in magnetic flux measured by the flux loop. The best comparison is with Flux Loop 1 which was closest to the plasma source and about 6 inches downstream of the location of the radial Bdot probe scan. The location of Flux Loop 1 is indicated in Figure 5.3. Flux Loop 1 consisted of a single loop 0.5m in diameter, or about 9.8 inches radius. The flux loop polarity was tested to ensure that increasing flux in the positive z direction (downstream) resulted in a postive voltage at the digitizer. The flux loop data was integrated to give a total change in magnetic flux for the same pulses that the radial scan was conducted. The results are shown in Figure 5.8. Figure 5.9 is a close up

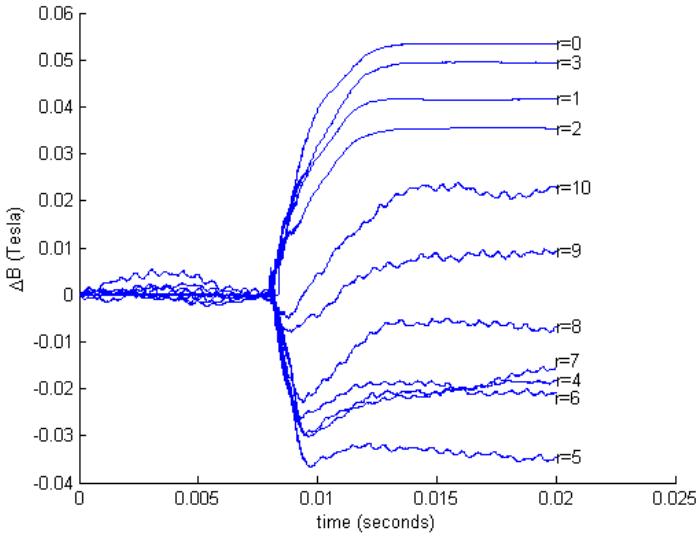

Figure 5.4: Change in magnetic field strength in the axial direction for several plasma pulses constituting a radial scan.

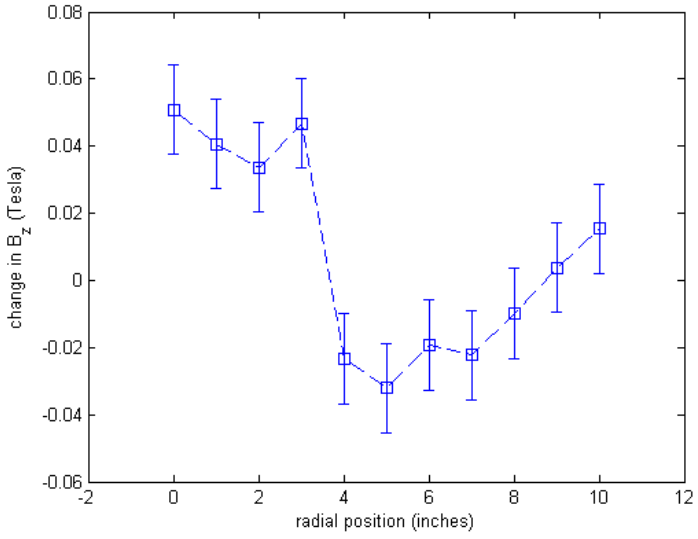

Figure 5.5: Radial profile of the change in the axial component of magnetic field strength.

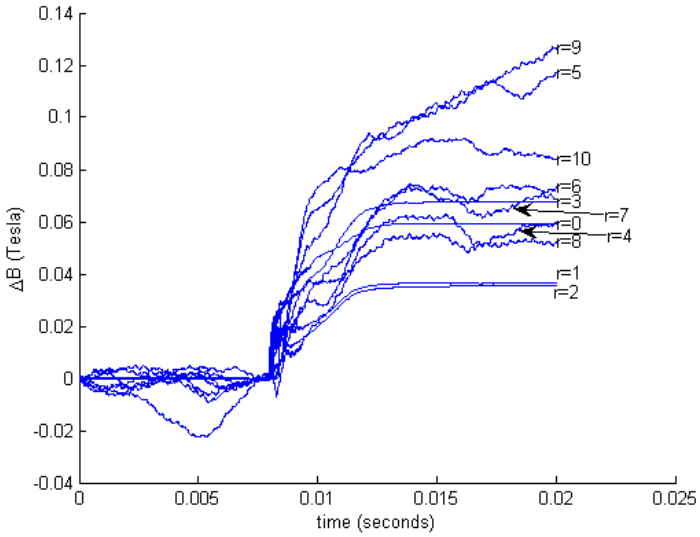

Figure 5.6: Change in magnetic field strength in the radial direction for several plasma pulses constituting a radial scan.

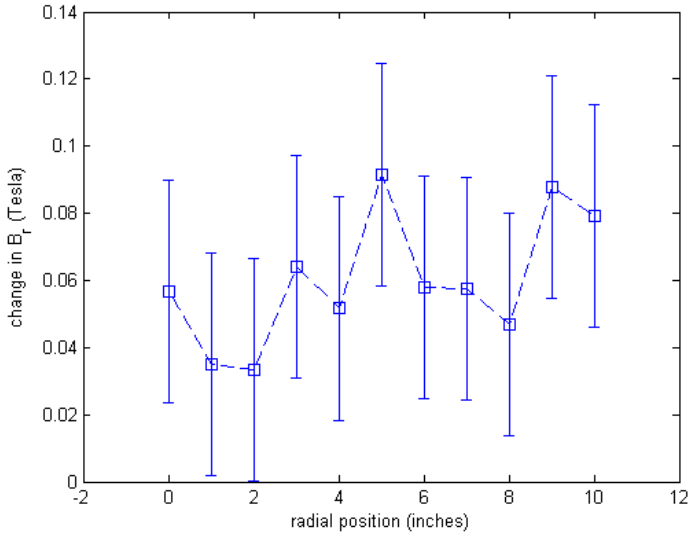

Figure 5.7: Radial profile of the change in the radial component of magnetic field strength.

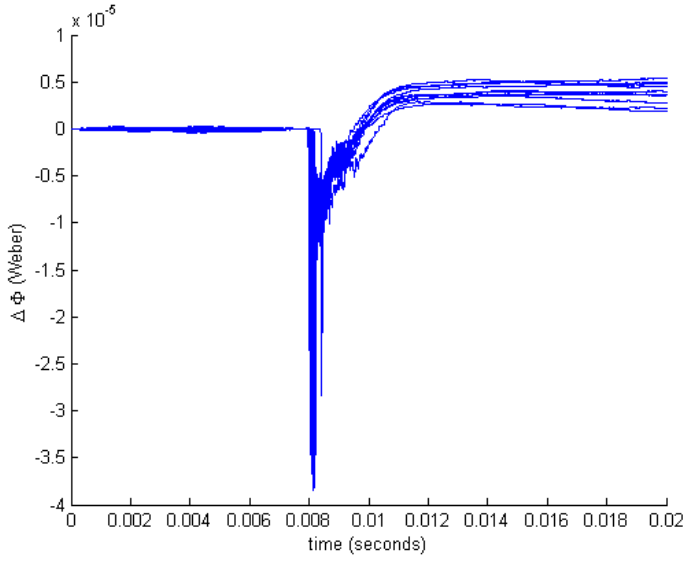

Figure 5.8: Integrated flux loop data giving change in total magnetic flux. These are the same pulses that comprise the radial scan in Figures 5.4 and 5.6.

of the time period near the plasma gun pulse. Because the flux loop encompassed a large area with respect to the magnetic field geometry, no attempt was made to reduce this to a magnetic field strength.

An assumption of cylindrical symmetry must be made in order to compare the integrated ΔB_z profile measured by the Bdot probe radial scan to the data from Flux Loop 1. This is probably not a very good assumption because the magnetic field perturbation should be related to the plasma density and Figure 4.1 clearly shows that the plasma density is somewhat off-center with respect to the vacuum chamber coordinate system. It would be preferable to perform the ΔB radial scan across the entire plasma plume. This would permit an examination of the cylindrical symmetry assumption. However, the probe construction and mounting technique did not leave sufficient room to scan the probe tip to the left of the machine's centerline.

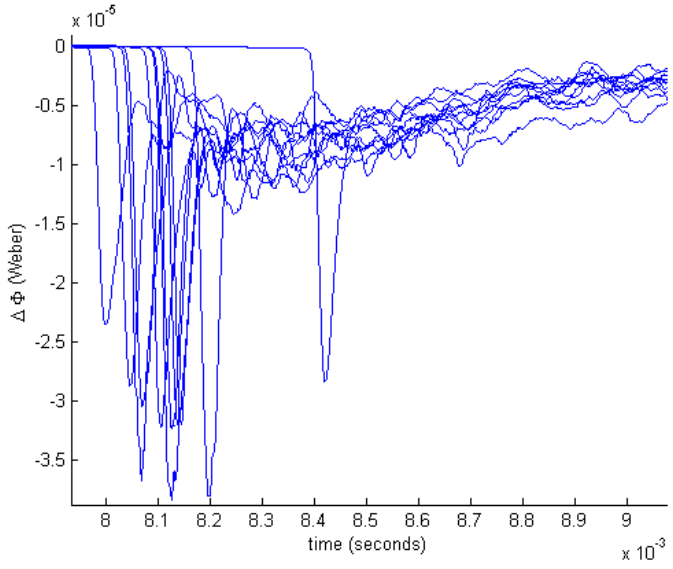

Figure 5.9: Small time scale behavior of changing magnetic flux for the same pulses displayed in Figure 5.8.

By assuming the total change in flux to be the initial peaks observed in Figure 5.9, the average total change in flux through flux loop one over the shots comprising the radial scan is -3.2×10^{-5} Weber and the standard deviation (used to estimate error) is 4.5×10^{-6}. An integral of revolution with the Bdot probe data results in a predicted total change in magnetic flux of -9.7×10^{-4} Weber. This agrees with the flux probe data in the direction of net change in flux, but differs by more than an order of magnitude. One should keep in mind the degree of repeatibility in the pulse data. This is again illustrated in Figure 5.9. Carrying the observed variation in magnetic field change through the cylindrical integration process shows that the error margin in the determination of total change in flux from the Bdot loop data is of the same order of magnitude as the result (1×10^{-3}).

The variability in plasma parameters over the course of the radial scan can be accounted for by scaling the Bdot loop data from the individual shots with another experimental

measurement that gives some indication of the overall quantity of interest. In the case of magnetic field measurements it is logical to use the encompassing flux loop as an indicator of the shot to shot variations in magnetic field effects. Figure 5.10 displays the results of multiplying the ΔB data from each shot of the radial scan with a scaling factor obtained by dividing the total change in flux observed from the flux loop by the average change in flux for the series of shots. This process is analagous to the data reduction algorithm used to compute a radial electron density profile by combining the data from the Langmuir probe scan and interferometer system. In that calculation the shot to shot variations in electron density that occur over the course of a multi-shot radial scan are accounted for by scaling the triple probe data with the variations in the line integrated electron density obtained from the microwave interferometer data. In both cases an instrument which effectively samples the entire cross section of the plume was used to interpret data from an instrument with a smaller spatial resolution. This technique allows the investigator to differentiate between global changes and local changes in the parameter of interest and makes possible a study of the detailed geometry of the system.

The density of the plasma created by the washer stack gun should determine the total magnetic flux that is carried along with the plasma. This is to be expected from the theoretical description of the detachment process because a more dense plasma will carry more magnetic flux along with it.

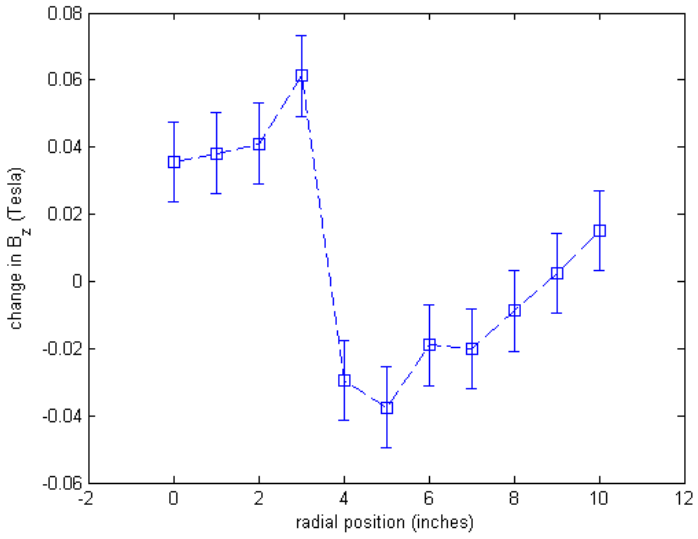

Figure 5.10: The radial scan data of Figure 5.4 rescaled to account for shot to shot variations in plasma source performance.

Chapter 6

Conclusions and Recommendations

One of the most important conclusions that can be drawn from this data is a knowledge of the effect of the plasma plume on the magnetic field. It is important to know whether the plasma drags the magnetic field along with it or is transported across the magnetic field lines. If it drags the field lines with it, then we can expect some sort of magnetic reconnection phenomena to show itself at some point in the plume. If the plasma drags the magnetic field along with it then it should be classified as a paramagnetic plasma. This means that it should cause the magnetic field to increase in the downstream direction and decrease in the radial direction.

What is actually observed is an increase in the magnetic field strength in the radial direction for all shots of the radial scan. This does not seem to support the hypothesis that the magnetic field is dragged along with the plasma.

The axial component of the magnetic field is more difficult to analyze. For positions closer to the axis, the change in B seems to point in the positive z direction (downstream). For positions farther from the axis, the change appears to point in the negative direction (upstream). This is evident in Figure 5.5. This observation could support the argument for a paramagnetic plasma in the exhaust if the assumption is made that the plasma column is only about 4 inches in radius at the position of the probe scan. This conclusion is supported by the measurements of plasma density depicted in Figure 4.1 which show an exhaust plume radius of about 10 cm.

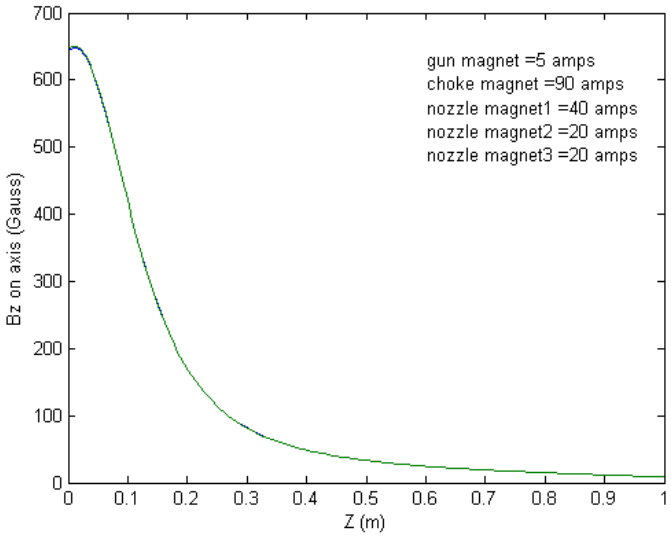

Figure 6.1: Axial magnetic field strength generated by the DDEX magnet coils.

The change in magnetic field should be compared with the predicted magnitude of the magnetic nozzle field. Figure 6.1 is a plot of axial magnetic field strength versus position. This magnetic field strength was calculated from the coil geometries and magnet coil currents used in the radial scan. Comparing this profile with the Bdot probe data shows that the change in magnetic field strength is almost equal to the maximum magnetic field generated at the plasma source. This would seem to indicate that the plasma drags almost all the magnetic field along with it through the nozzle. This observation does not agree with the prediction formula presented in Chapter 2.

The next step in this research would be searching for magnetic field perturbations in the exhaust of the VASIMR prototype VX-100. This is a 100kW version scheduled for operation beginning late 2007. Bdot probe construction should be optimized for the expected magnetic field transients in the large vacuum test chamber to be delivered summer 2007. Three axis Bdot probes should be attached to the translation stage in the chamber.

A thorough investigation of the magnetic field behavior in the detachment region would search for both singular changes in magnetic field strength when plasma is applied and high frequency oscillations in the magnetic field. This means that both small, single loop Bdot probes such as the ones made at KTH and larger, more sensitive probes for detecting ΔB will be necessary. These more sensitive coils should include active analog integration circuits in the probe design, such as the simple op-amp integrator suggested by Hutchinson.[15] The data from these probes should be combined with theoretical calculations of the vacuum magnetic field created by the coil set and experimental determination of field strength and direction using a three axis Hall probe mounted on a translation stage. The dominant detachment mechanism in the exhaust of the VASIMR engine still needs to be determined experimentally.

Bibliography

[1] Chang Díaz, F. R., "Progress on the VASIMR Engine," 39th AIAA/ASMA/SAE/ASEE Joint Propulsion Conference, Huntsville, AL July 20-23 2003.

[2] Glover, T. W., Chang Díaz, F. R., Squire, J. P., Jacobson, V. P., Chavers, D. G., and Carter, M. D., "Principal VASIMR Results and Present Objectives," Space Technology and Applications International Forum, Albuquerque NM 2005.

[3] Chang Díaz, F. R., et al., "The VASIMR Engine: Project Status and Recent Accomplishments," AIAA Paper 2004-0150, 2004.

[4] Chang Díaz, F. R., "The Development of the VASIMR Engine," *The International Conference of Electromagnetics in Advanced Space Applications*, Torino, Italy, September 13-17, 1999.

[5] Chang Díaz, F. R., "An Overview of the VASIMR Engine: High Power Space Propulsion with RF Plasma Generation and Heating," RADIO FREQUENCY POWER IN PLASMAS, 14th Topical Conference, Oxnard, CA, American Institute of Physics Conference Proceedings 595, 3 (2001).

[6] Chang Díaz, F. R., "The VASIMR Rocket," *Scientific American*, November, 2000, pp. 90-97.

[7] Chavers, D. G., et al, "Status of Magnetic Nozzle and Plasma Detachment Experiment," *AIAA Space Technology and Applications International Forum*, Albuquerque, New Mexico, February 2006.

[8] Arefiev, A. V., and Breizman, B. N., "Magnetohydrodynamic scenario of plasma detachment in a magnetic nozzle," *Physics of Plasmas*, Vol. 12, No. 043504, 2005.

[9] Hurtig, T., Brenning, N., and Raadu, M. A., "The role of high frequency oscillations in the penetration of plasma clouds across magnetic boundaries," *Physics of Plasmas*, Vol. 12, No. 012308, 2005.

[10] Ilin, A. V., Chang Díaz, F. R., Squire, J. P., Tarditi, A. G., Breizman, B. N., and Carter, M. D., "Simulations of Plasma Detachment in VASIMR," AIAA Paper 2002-0346, January 2002.

[11] Chen, F. F., *Introduction to Plasma Physics and Controlled Fusion*, Vol. 1, 2nd ed., Plenum Press, New York, 1984.

[12] Griffiths, D. J., "Electrodynamics," *Introduction to Electrodynamics*, 3rd ed., Prentice Hall, Upper Saddle River, New Jersey, 1999, pp. 301-306.

[13] Gesto, F., Blackwell, B., Charles, C., and Boswell, R., "Ion Detachment in the Helicon Double-Layer Thruster Exhaust Beam," *Journal of Propulsion and Power*, Vol. 22, No. 1, 2006.

[14] Swanson, D. G., "Waves in Fluid Plasmas," *Plasma Waves*, 2nd ed., Institute of Physics Publishing, Philadelphia, 2003, pp. 99-103.

[15] Hutchinson, I. H., "Magnetic Diagnostics," *Plasma Diagnostics*, Cambridge University Press, Cambridge, 1987, pp. 10-12.

[16] Beiersdorfer, P., and Clothiaux, E., "High-frequency magnetic measurements using small inductive probes," *American Journal of Physics*, Vol. 51, No. 11, 1983.

[17] Dobson, C. C., Jones, J. E., and Chavers, D. G., "Instrument reflections and scene amplitude modulation in a polychromatic microwave quadrature interferometer," *Review of Scientific Instruments*, 2004, Vol. 75, pp. 674-683.

[18] Deline, C., Chavers, D. G., Gilchrist, B., "Physics of Plasma Detachment in a Magnetic Nozzle," *AIAA Joint Propulsion Conference*, Sacramento, California, July 2006.

[19] Coleman, H. W., and Steele, W. G., Jr., *Experimentation and Uncertainty Analysis for Engineers*, John Wiley and Sons, Inc., 1999.